Acta Cryst. (1980). B36, 575–586

X-ray and Neutron Studies of a Displacive Phase Transition in *N,N*-Dimethylnitramine (DMN)

BY ALAIN FILHOL

*Laboratoire de Cristallographie et de Physique Cristalline, LA*144, *Université de Bordeaux* I, 351 *cours de la Libération,* 33405 *Talence, France, and Institut Laue–Langevin,* 156*X,* 38042 *Grenoble CEDEX, France*

GEORGES BRAVIC

*Laboratoire de Cristallographie et de Physique Cristalline, LA*144, *Université de Bordeaux* I, 351 *cours de la Libération,* 33405 *Talence, France*

MADELEINE REY-LAFON

*Laboratoire de Spectroscopie Infrarouge et Raman, LA*124, *Université de Bordeaux* I, 351 *cours de la Libération,* 33405 *Talence, France*

AND MICHEL THOMAS

Institut Laue–Langevin, 156*X,* 38042 *Grenoble CEDEX, France*

(*Received* 17 *July* 1979; *accepted* 5 *November* 1979)

Abstract

N,N-Dimethylnitramine has a phase transition at 107 K for the hydrogenated compound and 111 K for the deuterated compound, associated with a soft mode previously observed by Raman spectroscopy at low temperature. The purpose of this work is to determine the structural modifications at the transition. Powder diffraction patterns (120, 95, 15 K) and rotating-crystal and Weissenberg photographs (155, 95 K) obtained with neutrons show the existence of a superlattice corresponding to a doubling of the lattice below the transition temperature. The structures at 300, 180, 125 K (X-rays) and 125, 91, 85 K (neutrons) have been determined. The structural modifications between the high-temperature form (space group $P2_1/m$, $Z = 2$, planar molecule) and low-temperature form ($P2_1/c$, $Z = 4$, deformed molecule) can essentially be described by a rotation of the whole molecule ($\simeq 4°$ at $T_t - 20$ K) plus an intramolecular deformation: the N–N bond and the C–N–C plane form an angle of about 10° at $T_t - 20$ K.

Introduction

N-Nitrodimethylamine, usually called *N,N*-dimethylnitramine (DMN), belongs to the family of nitramines $\begin{matrix} R' \\ R \end{matrix}\!\!>\!N_A\!-\!N_BO_2$ which have provided some of the most common explosives and propellants.

DMN is interesting for several reasons. It is one of the simplest nitramines to be solid at ambient temperature (T_m = 331 K). It is not explosive whereas molecules such as hexahydro-1,3,5-trinitro-1,3,5-triazine (hexogen or RDX) or octahydro-1,3,5,7-tetranitro-1,3,5,7-tetrazocine (octogen or HMX), which are to some extent cyclic polymers of DMN, of three and four links respectively, are excellent secondary explosives.

Its conformation in the solid state is unlike that of the other nitramines whose structures are known. In fact, according to Costain & Cox (1947) and Krebs, Mandt, Cobbledick & Small (1979), at ambient temperature the skeleton of the DMN molecule is planar, whereas for other nitramines there is a more or less pronounced rotation of the NO_2 group around the N–N bond and a substantial angle (δ) between the CH_3–N_A–CH_3 plane and the N–NO_2 bond (up to respectively 10 and 51°). A certain mutual dependence between d_{N-N} and δ is also noted (Filhol *et al.*, 1971).

Finally, Rey-Lafon & Lagnier (1975*a*,*b*) have shown, by calorimetry and Raman spectroscopy, that DMN has a phase transition at T_t = 107 K, a transition involving very little energy (ΔS = 0·17 J K^{-1} mol^{-1}), which is reversible and non-destructive for the crystal. This transition is accompanied by a soft mode, which implies a displacive character. In addition, Rey-Lafon (1979) has shown that Raman spectra on oriented single crystals in the low-temperature phase suggest the existence of a superlattice for this phase. For the deuterated compound, this specific anomaly has been

0567-7408/80/030575-12$01.00

observed at 111 K (Lagnier, 1978) and the soft mode also exists.

Only a few transitions associated with a soft mode have been described for molecular crystals: chloranil (Terauchi, Sakai & Chihara, 1975; Hanson, 1975; Ellenson & Kjems, 1977) and biphenyl (Bree & Edelson, 1977; Cailleau, Baudour & Zeyen, 1979; Cailleau, Moussa & Mons, 1979) may be cited.

The study presented here is of the structural nature of the DMN phase transition. This work has been carried out independently of Krebs *et al.* (1979) and, for the high-temperature phase, includes some crystallographic results similar to those already published. It should also be mentioned that the following results refer to samples that are either hydrogenated ($DMN\text{-}H_6$) or deuterated ($DMN\text{-}D_6$). As the behavior of these two compounds is very similar, the results will generally be discussed together.

Experimental

The study of the phase transition of DMN has necessitated various radiocrystallographic analysis techniques. In general, the use of X-rays has given disappointing results because the cold-nitrogen gas-flow cryostats used (powder diffractometer, Guinier–Lehnne camera, four-circle diffractometer) did not permit a clear and steady crossing of the transition temperature. The use of neutrons has eliminated this difficulty (helium cryostat) and has made it possible to specify the behavior of the methyl groups in this compound.

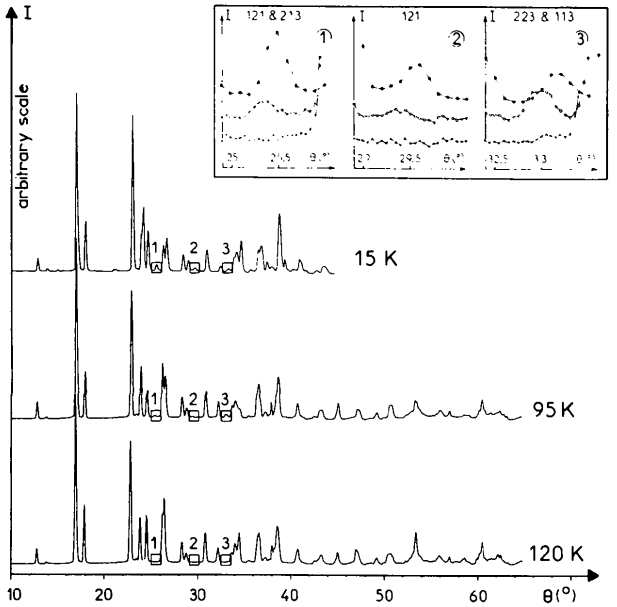

Fig. 1. Neutron diffraction powder patterns of $DMN\text{-}D_6$ at 120, 95 and 15 K (λ = 2·397 Å). The inset shows the first three visible superlattice reflections.

(i) *Samples*

The hydrogenated compound ($DMN\text{-}H_6$) and the deuterated compound ($DMN\text{-}D_6$) were kindly supplied by Mr Michaud (CEA-Vaujour, France). Crystals with volumes of several mm^3 suitable for neutron experiments were obtained by cleavage and chemical erosion of crystals several cm^3 in volume grown by a zone-melting method (Bridgman method).

(ii) *Neutron diffraction on powder*

The powder diagrams of $DMN\text{-}D_6$ at 120, 95 and 15 K (Fig. 1) were recorded on the multicounter diffractometer D1B at the ILL, Grenoble. The incident neutron beam had a wavelength of 2·397 (2) Å [graphite monochromator (002) in reflection] and a flux of approximately $1{\cdot}5 \times 10^4$ n mm^{-2} s^{-1} at the sample position. The sample, consisting of 1500 mm^3 powder enclosed in a vanadium tube of 7 mm diameter, was placed in a liquid-helium cryostat.

With an intrinsic resolution of the multicounter of 0·1° (Bragg angle 2θ), the spectra at 120 and 95 K were recorded for two multicounter positions staggered by half an interval between cells in order to obtain a final resolution of 0·05°.

The positions of the peaks, well separated or partially overlapping, were determined by the Gaussian summation method (program *INTEGR* of P. Wolfers & J. L. Soubeyroux, ILL, Grenoble).

(iii) *Rotating-crystal and neutron Weissenberg photographs*

The neutron rotating-crystal photographs (exposure time 3 h) and the neutron Weissenberg photographs of the levels *h*0*l*, *h*1*l*, *h*2*l* (exposure time 11 h) of $DMN\text{-}D_6$ at 155 and 90 K (Fig. 2) were obtained on the ILL D12 instrument, a normal-beam-geometry Weissenberg camera with a vertical rotation axis (Hohlwein & Wright, 1980).

The sample was a quasi-spherical single crystal of $DMN\text{-}D_6$, approximately 2 mm in diameter. It was placed in a liquid-helium cryostat. The substantial parasitic scattering produced by the aluminum walls was eliminated by oscillating radial Soller slits, inserted between the photographic film and the tail of the cryostat (Wright & Berneron, 1980).

The incident neutron beam had a flux of approximately 10^4 n mm^{-2} s^{-1} at the sample position for a wavelength of 1·69 Å [graphite monochromator (002) in reflection].

(iv) *X-ray diffraction on single crystals*

Measurements were carried out on an automatic AED-Siemens diffractometer at the ILL. The cryogenic device was a nitrogen gas-flow system. The experi-

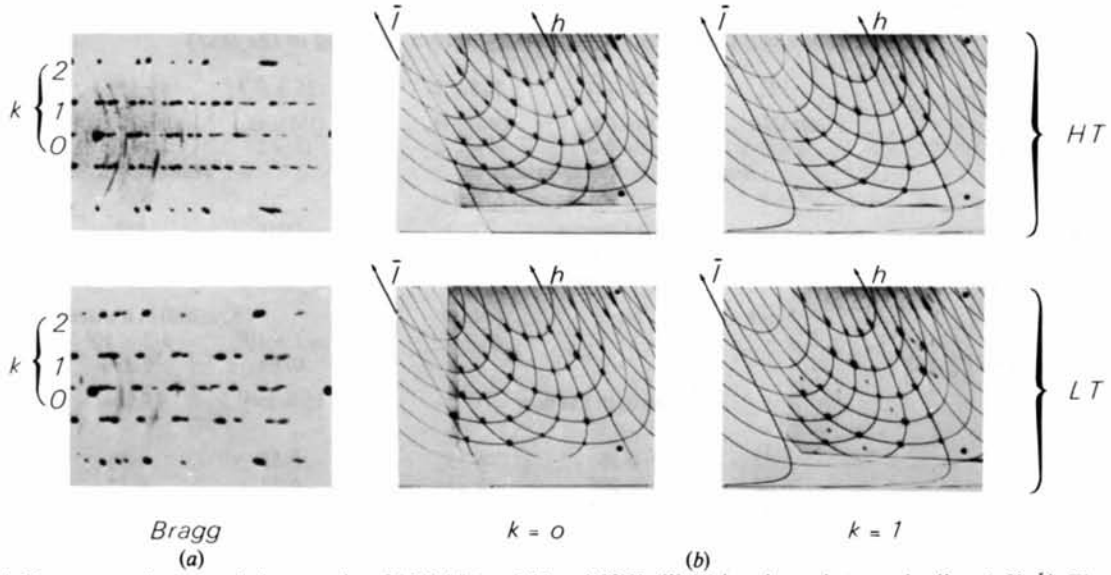

Fig. 2. (*a*) Neutron rotating-crystal photographs of DMN-D_6 at 155 and 90 K. (*b*) Weissenberg photographs (λ = 1·69 Å). The diffuse lines in the form of arcs observable on the rotation photographs are due to the scattering of neutrons by the aluminium cryostat walls. The horizontal stripes visible on one of the Weissenberg photographs are due to a failure of the oscillation movement of the radial Soller slits.

mental conditions are indicated in Table 1. At each temperature the lattice parameters were calculated from the Eulerian angles observed for about ten strong reflections. Only the data measured at 293 K had to be corrected for the falling-off of intensities with time; this can certainly be attributed to the radiolysis of the compound by X-rays. In fact, some nitramines are known for being highly sensitive to radiation at ambient temperature but the decomposition products are trapped in the lattice at low temperature.

(v) *Neutron diffraction on single crystals*

For all these measurements, the experimental conditions are indicated in Table 1 and commented on below.

The ILL diffractometer D10 is an automatic four-circle diffractometer installed on the thermal neutron guide H24 at the High Flux Reactor. The cryostat (Claudet, Tippe & Yelon, 1976) was a helium gas-flow device with a spherical aluminum double shell, centered in the Eulerian cradle. The attenuation of the neutron beam by the walls was therefore low and independent of the crystal orientation.

The lattice parameters were calculated from the Eulerian angles observed for 15 strong reflections at 125 K and 21 at 85 K. They are relatively imprecise because of a significant eccentricity of the crystal, which, for technical reasons, could not be corrected.

The measurements carried out at 85 K did not include the collection of superlattice reflections, because their existence was not known at the time of the experiment.

The D8 diffractometer is also an automatic four-circle diffractometer, but installed at the end of the H11 High Flux thermal neutron beam tube at the HFR. A Displex CSA 1003C Air Products cryorefrigerator was used, with the sample cooled by conduction in a cylindrical container full of gaseous helium. The transmission factor (t) of the walls (aluminum and vanadium) was thus a function of the angles ω and χ of the diffractometer ($t = 0{\cdot}975$ for $\chi = 0°$) and the data have therefore been corrected for the corresponding absorption.

The lattice parameters at 296, 180, 91, 73 K were calculated from the Eulerian angles observed for about 20 strong reflections.

The superlattice reflection $\bar{3}11$ of DMN-D_6 was measured on the D8 diffractometer by $\omega/2\theta$ step scans, with decreasing temperature in the interval 137 to 76 K. For these shorter measurements, the Displex cryorefrigerator guaranteed a sample temperature stable to better than $\pm 0{\cdot}2$ K. The absolute value was calibrated by reference to the ferroelectric transition (T_t = 122·4 K) of a single crystal of KH_2PO_4.

Results

(i) *Evidence of the phase transition*

Overall, the powder diagrams obtained with neutrons for DMN-D_6 at 120 K (high-temperature form: HT)

Table 1. *Bragg diffraction measurements on single crystals with automatic four-circle diffractometers: experimental conditions and final R factors (defined in the text)*

Temperature (K)	293	180 ± 2	125 ± 2	125 ± 0·2	91 ± 0·5	85 ± 0·2
Sample	DMN-H_6	DMN-H_6	DMN-H_6	DMN-H_6	DMN-D_6	DMN-H_6
Dimensions (mm)	$\varnothing \simeq 0{\cdot}2$	$\varnothing \simeq 0{\cdot}2$	$\varnothing \simeq 0{\cdot}2$	$\varnothing \simeq 2$	$\varnothing \simeq 2$	$\varnothing \simeq 2$
Mounted in	Sealed Lindemann-glass tube				Sealed quartz tube	
Vertical axis	$\simeq a$	$\simeq a$	$\simeq a$	–	$\simeq b$	–
Diffractometer	AED Siemens			D10	D8	D10
Radiation	X-rays			Neutrons	Neutrons	Neutrons
Wavelength: λ (Å)	Cu $K\alpha$ (Ni filtered)			1·436 (1)	1·1405 (3)	1·436 (1)
Monochromator	None	None	None	Cu(200) in transmission		
Flux (n mm^{-2} s^{-1})	–	–	–	$\simeq 1 \times 10^4$	$5{\cdot}3 \times 10^5$	$\simeq 1 \times 10^4$
$\lambda/2$ contamination $F^2_{\lambda/2}/F^2_{\lambda}$	–	–	–	0·1%	0·2%	0·1%
Cryostat	Cold-nitrogen gas flow			Helium[1]	Displex	Helium[1]
Lattice[5]						
a (Å)	6·58	6·56	6·55	6·55	6·54	6·54
b (Å)	6·50	6·295	6·23	6·23	6·18	6·195
c (Å)	6·13	6·095	6·08	6·08	12·14	6·06, 12·12
β (°)	123·07	123·55	123·60	123·60	123·80	123·65
Space group	$P2_1/m$	$P2_1/m$	$P2_1/m$	$P2_1/m$	$P2_1/c$	$P2_1/m$, $P2_1/c$
Z	2	2	2	2	4	2 4
Intensity measurements						
Scan mode	$\omega/2\theta$	$\omega/2\theta$	$\omega/2\theta$	ω	$\omega/2\theta$	ω
Scan type	Five-points method[3]				Step scan	
Fraction of reciprocal space measured	$\frac{1}{2}$	$\frac{1}{2}$	$\frac{1}{2}$	$\frac{1}{4}$	$\frac{1}{4}$	$\frac{1}{4}$
$(\sin\theta/\lambda)_{max}$ (Å^{-1})	0·613	0·613	0·613	0·654	0·671	0·654
Date reduction					$\sigma(I)/I$ criterion[4]	
Absorption: μ_{cal} (mm^{-1})	1·05	1·05	1·05	$\simeq 0{\cdot}3$	$\simeq 0{\cdot}1$	$\simeq 0{\cdot}3$
Number of independent reflections						
Total	402	443	447	535	1039	419[2]
$F_o > 3\sigma(F_o)$		415	435	386	1029	320
$R(F_o)$	0·046	0·051	0·040	0·036	0·057	0·039, 0·036
$R(F_o$ superlattice reflections)					0·059	

(1) Claudet, Tippe & Yelon (1976). (2) The superlattice reflections were not measured. (3) Troughton (1969). (4) Lehmann & Larsen (1974). (5) Cell dimensions calculated from data (Fig. 9) and used for structure refinements.

and at 95 and 15 K (low-temperature form: LT) are very similar (Fig. 1) with, however, the following differences. An increase of 10% at 95 K and of 20% at 15 K is noted for the half-widths of peaks with respect to the observations at 120 K. Some diffraction peaks present noticeable variations in intensity. Finally, on the spectra at 95 and 15 K, the presence of a small number of low-intensity additional reflections was noted which could not be indexed on the basis of lattice parameters extrapolated from values already determined for higher temperatures.

These results therefore suggest, in agreement with those of Raman spectroscopy (Rey-Lafon, 1979), the existence of a superlattice for the LT form of DMN.

These initial observations are amply confirmed by the analysis of the neutron rotating-crystal and Weissenberg photographs obtained at 155 K (HT) and 95 K (LT) for DMN-D_6 (Fig. 2).

In fact, the rotating-crystal photograph at 95 K does not show Bragg reflections or diffuse scattering outside the layers observed on the photograph at 155 K. On the other hand, it shows the $k \neq 0$ layers with a larger number of diffraction spots. The Weissenberg photographs of the reciprocal levels $h0l$, $h1l$ and $h2l$ of DMN-D_6 at 155 and 95 K indicate the nature of the crystal-lattice modification associated with the transition: on the photographs at 95 K, diffraction spots of low intensity appear, which, in the lattice (I) defined by Costain & Cox (1947) and Krebs *et al.* (1979), are of the type $h_I = n + \frac{1}{2}$, $k_I \neq 0$, $l_I = n' + \frac{1}{2}$ (where n and n' are integers).

The corresponding lattice transformation is more simply expressed in lattice (II) as defined in Fig. 3. There is a transition from the HT lattice to the LT lattice by the doubling of the direct cell parameter c_{II} accompanied by the loss of a mirror which becomes a

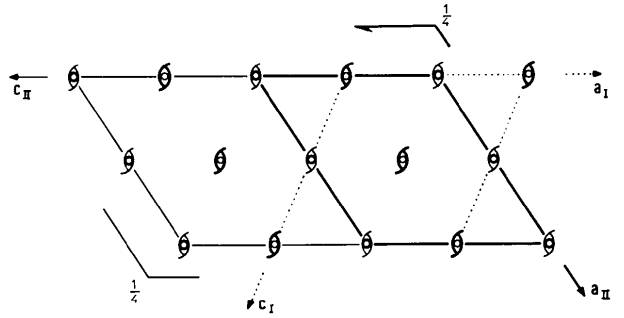

Fig. 3. Definition of the cell. Lattice (I) is represented by dotted lines, lattice (II) is represented by continuous lines; in both cases heavy lines are for the HT and light lines for the LT form. Only the symmetry elements shown in heavy lines are kept in the LT phase.

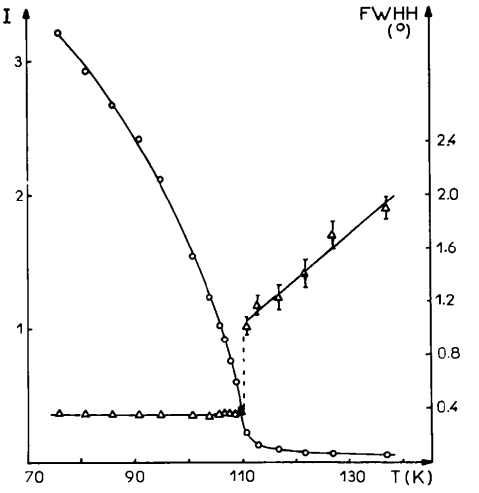

Fig. 4. Changes as a function of temperature in the superlattice reflection $\bar{3}11$. O Integrated intensity, △ full width at half-height.

glide plane, and the loss of alternately a center of inversion or a 2_1 axis in the c direction.

In these conditions, the space group, which was $P2_1/m$ with $Z = 2$ in the HT phase, becomes $P2_1/c$ with $Z = 4$ for the LT phase.

The relationships as regards passage from (I) to (II) for the atomic coordinates x,y,z and for the Miller indices h,k,l of the reflections are:

$$x_{II} = z_I \qquad h_{II} = -h_I - l_I$$
$$y_{II} = y_I \qquad k_{II} = k_I$$
$$mz_{II} = \tfrac{1}{2} - x_I + z_I \qquad l_{II} = mh_I$$

with $m = 1$ for the HT phase and $m = 2$ for the LT phase. For the sake of clarity, only (II) will be used below, including when reference is made to results obtained by other authors.

(ii) *Determination of structures*

The structure of the HT form was determined with *MULTAN* (Germain, Main & Woolfson, 1971) from X-ray diffraction data of DMN-H_6 at 293 K and is identical to that described by Krebs *et al.* (1979).

The least-squares refinement of the structure found by X-rays (293, 180, 125 K) and neutrons (125 K) was carried out by minimizing $\sum w(|F_o| - |F_c|)^2$ with $w^{1/2} = (a + |F_o| + c|F_o|^2)^{-1/2}$, $a = 2|F_o|_{min}$, $c = 2/|F_o|_{max}$.

Scattering factors (X-rays) were taken from *International Tables for X-ray Crystallography* (1974) for C, N and O, and from Stewart, Davidson & Simpson (1965) for H. The Fermi lengths (10^{-14} m) are $b_C = 0{\cdot}665$, $b_N = 0{\cdot}938$, $b_O = 0{\cdot}577$, $b_H = -0{\cdot}378$, $b_D = 0{\cdot}667$. The final values of $R = \sum(||F_o| - |F_c||)/\sum|F_o|$ are given in Table 1.

Difference maps made at the final stage of each refinement showed no significant peaks.

The structure of the LT form was determined by the multisolution method, starting from the diffraction data for neutrons for DMN-D_6 at 91 K and taking account of the information on the signs (s) of the F_c values of the main reflections (r_m) given by the structure of the HT form, *i.e.* $l = 4n$, $s_{LT} = s_{HT}$; $l = 4n + 2$, $s_{LT} = \varepsilon s_{HT}$ with ε = plus or minus but identical for all reflections of this type.

The least-squares refinement was carried out by applying independent scale factors k_m and k_s to all the r_m reflections on the one hand, and the superlattice reflections (r_s) on the other. Although the intensity of the superlattice reflection $\bar{3}11$ still increased at temperatures below 91 K (Fig. 4), the refinement led to $k_s/k_m = 1$, and not to a value different from 1 as is the case for biphenyl (Cailleau, Baudour & Zeyen, 1979).

The data on DMN-H_6 at 85 K are unfortunately incomplete as the superlattice reflections were not measured. A first refinement was therefore carried out in the space group $P2_1/m$ (HT form). It converged without difficulty ($R = 0{\cdot}039$) and gave an average description of the DMN-H_6 (LT form) over two symmetrical positions on either side of the pseudo-mirror introduced in this way. In a second refinement, the atomic positions obtained for DMN-D_6 at 91 K were used as starting parameters in $P2_1/c$. It also converged rapidly ($R = 0{\cdot}036$) and therefore gave the true description of the DMN-H_6 structure at 85 K.

For all refinements, the final atomic coordinates are given in Table 2, and the bond lengths and angles in Table 3.* Fig. 5 shows the crystal packing for DMN-D_6 at 91 K.

* Lists of structure factors and thermal parameters have been deposited with the British Library Lending Division as Supplementary Publication No. SUP 34816 (34 pp.). Copies may be obtained through The Executive Secretary, International Union of Crystallography, 5 Abbey Square, Chester CH1 2HU, England.

Table 2. *Fractional coordinates with e.s.d.'s in parentheses and isotropic thermal parameters* (Å²)

(*a*) X-rays at 293 K; (*b*) X-rays at 180 K; (*c*) X-rays at 125 K; (*d*) Neutrons at 125 K; (*e*) Neutrons at 91 K; (*f*) neutrons at 85 K; (*g*) neutrons at 85 K. $P2_1/m$ refinement. The maximum e.s.d.'s of isotropic thermal parameters are 1 Å² for hydrogen atoms from X-ray data and 0·2 Å² in other cases.

		x	*y*	*z*	*B*
O(1)	*a*	0·4503 (4)	0·25	0·3781 (4)	6·4
	b	0·4485 (5)	0·25	0·3784 (5)	3·4
	c	0·4476 (3)	0·25	0·3777 (3)	3·1
	d	0·4490 (5)	0·25	0·3792 (5)	2·1
	e	0·4468 (4)	0·2814 (4)	0·1887 (2)	1·0
	f	0·4479 (5)	0·2812 (6)	0·1895 (3)	1·1
	g	0·4480 (6)	0·25	0·3790 (5)	2·4
O(2)	*a*	0·8418 (4)	0·25	0·6435 (4)	5·9
	b	0·8456 (4)	0·25	0·6538 (5)	3·0
	c	0·8462 (3)	0·25	0·6560 (3)	2·7
	d	0·8460 (5)	0·25	0·6571 (5)	1·6
	e	0·8469 (4)	0·2617 (4)	0·3296 (2)	0·9
	f	0·8459 (5)	0·2672 (9)	0·3283 (3)	0·9
	g	0·8461 (5)	0·25	0·6571 (5)	1·3
N(1)	*a*	0·6125 (4)	0·25	0·8010 (4)	4·4
	b	0·6093 (5)	0·25	0·8070 (5)	2·4
	c	0·6076 (3)	0·25	0·8061 (4)	2·2
	d	0·6069 (3)	0·25	0·8060 (3)	1·4
	e	0·6056 (2)	0·2705 (2)	0·4034 (1)	0·7
	f	0·6065 (3)	0·2728 (4)	0·4035 (1)	0·7
	g	0·6065 (3)	0·25	0·8070 (3)	1·3
N(2)	*a*	0·6359 (4)	0·25	0·5984 (4)	4·5
	b	0·6352 (5)	0·25	0·6037 (6)	2·3
	c	0·6350 (3)	0·25	0·6060 (4)	2·2
	d	0·6345 (3)	0·25	0·6057 (3)	1·3
	e	0·6343 (2)	0·2708 (2)	0·3033 (1)	0·6
	f	0·6339 (3)	0·2727 (4)	0·3032 (1)	0·7
	g	0·6340 (3)	0·25	0·6064 (3)	1·3
C(1)	*a*	0·3678 (5)	0·25	0·7446 (6)	5·3
	b	0·3605 (6)	0·25	0·7435 (7)	2·8
	c	0·3585 (4)	0·25	0·7440 (5)	2·6
	d	0·3587 (4)	0·25	0·7442 (4)	1·6
	e	0·3557 (4)	0·2656 (3)	0·3713 (2)	0·8
	f	0·3554 (4)	0·2693 (7)	0·3710 (2)	0·9
	g	0·3557 (4)	0·25	0·7422 (5)	1·3
C(2)	*a*	0·8280 (6)	0·25	1·0577 (6)	5·6
	b	0·8275 (7)	0·25	1·0685 (7)	3·0
	c	0·8262 (4)	0·25	1·0707 (5)	2·7
	d	0·8260 (5)	0·25	1·0708 (4)	1·7
	e	0·8236 (4)	0·2384 (3)	0·5355 (2)	0·9
	f	0·8244 (4)	0·2335 (7)	0·5356 (2)	0·9
	g	0·8242 (4)	0·25	1·0710 (4)	1·3
H(1*A*)	*a*	0·376 (5)	0·25	0·896 (6)	7
	b	0·371 (8)	0·25	0·901 (9)	5
	c	0·368 (4)	0·25	0·912 (5)	3
	d	0·370 (1)	0·25	0·928 (1)	3·5
	e	0·3688 (5)	0·2703 (5)	0·4645 (5)	2·1
	f	0·369 (1)	0·280 (1)	0·4644 (6)	2·2
	g	0·368 (1)	0·25	0·929 (1)	3·2
H(1*B*)	*a*	0·276 (4)	0·126 (4)	0·640 (4)	7
	b	0·272 (5)	0·116 (5)	0·639 (5)	3
	c	0·270 (3)	0·121 (3)	0·642 (3)	3
	d	0·2605 (8)	0·1097 (8)	0·6295 (9)	3·5
	e	0·2620 (5)	0·1189 (5)	0·3173 (3)	2·1
	f	0·260 (1)	0·119 (2)	0·3171 (9)	2·6
	g	0·2573 (8)	0·1070 (8)	0·6272 (9)	2·9
H(1*C*)	*e*	0·2536 (5)	0·4053 (5)	0·3108 (3)	2·1
	f	0·255 (2)	0·403 (2)	0·3104 (9)	2·9
H(2*A*)	*a*	0·775 (6)	0·25	1·177 (7)	7
	b	0·785 (9)	0·25	1·19 (1)	5
	c	0·780 (5)	0·25	1·202 (5)	3
	d	0·769 (1)	0·25	1·207 (1)	3·0
	e	0·7675 (5)	0·2449 (5)	0·6042 (2)	1·8
	f	0·769 (1)	0·225 (1)	0·6043 (5)	1·9
	g	0·768 (1)	0·25	1·209 (1)	2·7
H(2*B*)	*a*	0·919 (4)	0·107 (4)	1·088 (5)	9
	b	0·922 (6)	0·111 (6)	1·104 (7)	6
	c	0·926 (3)	0·121 (4)	1·102 (4)	5
	d	0·935 (1)	0·110 (1)	1·103 (1)	5·1
	e	0·9044 (6)	0·0808 (5)	0·5432 (3)	2·7
	f	0·902 (1)	0·083 (2)	0·5436 (8)	2·6
	g	0·934 (1)	0·110 (1)	1·102 (1)	4·8
H(2*C*)	*e*	0·9580 (6)	0·3653 (6)	0·5599 (3)	2·9
	f	0·963 (1)	0·360 (2)	0·5570 (7)	2·6

(iii) *The DMN molecule in the HT and LT structures*

High-temperature form (HT): a detailed description of the structures at 293 and 143 K has been given by Krebs *et al.* (1979), so only certain important points will be discussed here.

All the atoms (except some H atoms) are in the crystallographic mirror. The symmetry of the molecule is strictly *m* and almost *mm*. The bond lengths and angles do not vary noticeably with temperature (Table 3). Intramolecular contacts, from neutron results for DMN-H_6 at 125 K, are: H(1*A*)···H(2*A*) = 2·191 (7), H(1*B*)···O(1) = 2·585 (7), H(2*B*)···O(2) = 2·589 (7) Å.

For this phase, the conformation of DMN is the same as that determined by Bastiansen (1950) and Stolevik & Rademacher (1969) by electron diffraction in the gaseous state with, however, differences in bond lengths and angles (Table 3). This is also the most stable conformation for the free molecule, as shown by the calculations of Farminer & Webb (1975) (approximation INDO) and Duke (1978) (*ab initio* MO).

Low-temperature form (LT): Fig. 6 shows the conformation of DMN below T_t. The N(1)–N(2) bond

Table 3. *Bond distances* (Å) *and angles* (°)

	Neutrons			X-rays				Electrons
	85 K	91 K (deuterated)	125 K	125 K	143 K*	180 K	293 K	Gas†
O(1)–N(2)	1·233 (5)	1·243 (3)	1·233 (5)	1·244 (4)	1·239 (3)	1·237 (5)	1·230 (4)	1·223 (2)
O(2)–N(2)	1·244 (5)	1·242 (3)	1·240 (4)	1·241 (4)	1·235 (3)	1·238 (5)	1·226 (4)	
N(1)–N(2)	1·323 (3)	1·328 (2)	1·326 (3)	1·324 (4)	1·329 (3)	1·341 (6)	1·332 (4)	1·382 (3)
N(1)–C(1)	1·461 (4)	1·453 (3)	1·452 (4)	1·457 (4)	1·453 (3)	1·455 (7)	1·451 (5)	1·460 (3)
N(1)–C(2)	1·457 (4)	1·449 (3)	1·447 (4)	1·445 (4)	1·446 (4)	1·440 (7)	1·432 (5)	
C(1)–H(1*A*)	1·09 (1)	1·086 (4)	1·078 (9)	0·99 (4)	0·97 (3)	0·92 (7)	0·90 (4)	1·121 (5)
C(1)–H(1*B*)	1·11 (1)	1·086 (4)	1·081 (7)	0·98 (2)	0·96 (2)	1·02 (4)	1·00 (3)	
C(1)–H(1*C*)	1·06 (1)	1·088 (4)						
C(2)–H(2*A*)	1·08 (1)	1·082 (4)	1·082 (9)	1·00 (4)	0·94 (3)	0·92 (7)	0·97 (5)	
C(2)–H(2*B*)	1·04 (1)	1·087 (5)	1·075 (8)	0·99 (3)	0·99 (2)	1·02 (4)	1·07 (3)	
C(2)–H(2*C*)	1·11 (1)	1·087 (5)						
N(2)–N(1)–C(1)	117·2 (2)	117·6 (2)	117·7 (2)	117·6 (3)	117·7 (2)	116·7 (4)	117·1 (3)	116·2 (6)
N(2)–N(1)–C(2)	117·5 (2)	117·4 (2)	117·8 (2)	117·9 (3)	117·7 (2)	117·9 (4)	118·4 (3)	
C(1)–N(1)–C(2)	124·2 (3)	124·1 (2)	124·5 (2)	124·5 (3)	124·6 (2)	125·3 (4)	124·5 (3)	127·6 (6)
O(1)–N(2)–O(2)	123·3 (3)	123·8 (2)	123·7 (3)	123·4 (3)	124·0 (2)	124·0 (4)	124·0 (3)	130·4 (6)
O(1)–N(2)–N(1)	118·3 (3)	118·1 (2)	118·3 (3)	118·3 (3)	117·7 (2)	118·3 (4)	118·2 (3)	114·8 (6)
O(2)–N(2)–N(1)	118·4 (3)	118·1 (2)	118·0 (3)	118·3 (3)	118·3 (2)	117·7 (4)	117·8 (3)	
N(1)–C(1)–H(1*A*)	106·7 (5)	107·1 (3)	107·9 (5)	108 (2)	106 (2)	107 (4)	109 (3)	102
N(1)–C(1)–H(1*B*)	110·6 (7)	110·6 (3)	110·4 (4)	110 (1)	112 (1)	109 (2)	111 (2)	
N(1)–C(1)–H(1*C*)	110·3 (7)	109·9 (3)						
H(1*A*)–C(1)–H(1*B*)	111·0 (8)	110·0 (4)	110·1 (6)	109 (2)	110 (2)	110 (5)	110 (3)	
H(1*A*)–C(1)–H(1*C*)	109·6 (9)	110·2 (4)						
H(1*B*)–C(1)–H(1*C*)	109 (1)	109·0 (4)	108·0 (5)	109 (2)	107 (1)	111 (3)	107 (2)	
N(1)–C(2)–H(2*A*)	108·3 (5)	107·6 (3)	107·6 (5)	110 (2)	108 (2)	109 (4)	106 (2)	
N(1)–C(2)–H(2*B*)	112·4 (7)	110·5 (3)	110·6 (5)	111 (2)	110 (1)	110 (3)	108 (2)	
N(1)–C(2)–H(2*C*)	108·1 (6)	110·5 (3)						
H(2*A*)–C(2)–H(2*B*)	103·9 (8)	108·9 (4)	109·8 (6)	108 (3)	106 (2)	104 (5)	106 (3)	
H(2*A*)–C(2)–H(2*C*)	115·7 (8)	109·3 (4)						
H(2*B*)–C(2)–H(2*C*)	108·5 (9)	110·0 (4)	108·5 (6)	109 (2)	116 (2)	117 (4)	121 (2)	

* Krebs *et al.* (1979).
† Stolevik & Rademacher (1969).

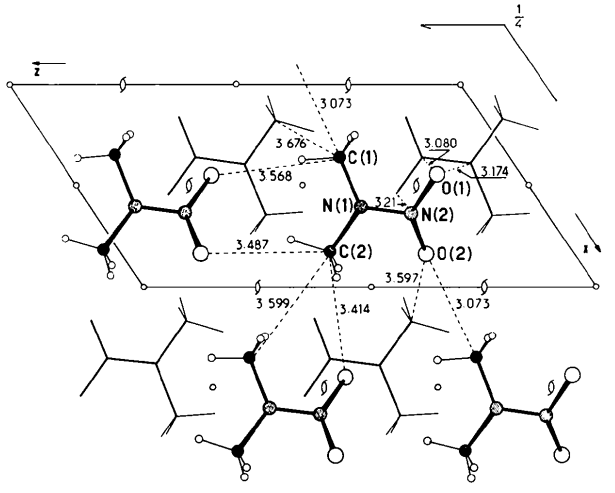

Fig. 5. Projection of the structure of DMN-D_6 at 91 K parallel to *b*, with some intermolecular contacts (Å) (average e.s.d. 0·003 Å).

forms an angle δ with the plane C(1)–N(1)–C(2), while the NO_2 torsion angle α_t around N(1)–N(2) is almost zero (Table 4). In the folding back of the molecule which occurs at the level of N(1), atoms H(1*A*) and H(2*A*) remain respectively in the planes defined by N(2)–N(1)–C(1) and N(2)–N(1)–C(2) while H(1*B*), H(1*C*) and H(2*B*), H(2*C*) are symmetrically disposed about the respective planes. Bond lengths and angles other than those of N(1) remain practically unchanged in relation to the values of the HT form (Table 3). When the phase transition occurs, the molecule loses its *m* symmetry and passes from having *mm* pseudo-symmetry (HT) to *m* pseudo-symmetry (LT).

This new conformation of DMN is in fact more in line with properties of the nitramine group determined from a survey of the available structural data on other compounds (Filhol, 1971).

As regards the displacement of the molecule in the lattice when passing from the HT to the LT form, the center of gravity (*G*) of the molecule is slightly

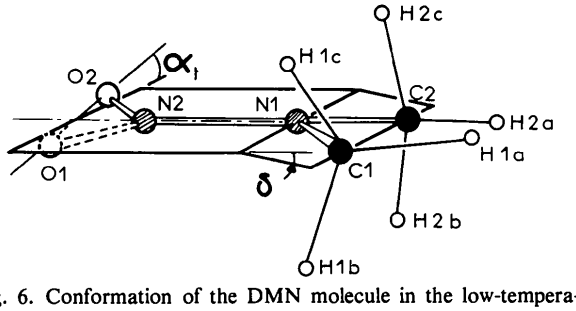

Fig. 6. Conformation of the DMN molecule in the low-temperature phase.

Table 4. *Values of parameters describing the molecular deformations and displacements*

δ: angle between plane CH_3–N(1)–CH_3 and bond N(1)–N(2) [similar to the dihedral angle between planes CH_3–N(1)–CH_3 and N(1)–N(2)–O(2) if α_t is small].
ω: molecular rotation around the a axis, defined as the angle between b and [C(1)–C(2) ∧ N(1)–N(2)].
α_t: torsion angle defined as the angle of the projections along N(1)–N(2) of C(1)–C(2) and O(1)–O(2).
t_G: distance from the center of mass of the molecule to the symmetry plane.

	T(K)	$T-T_t$(K)	δ(°)	α_t(°)	ω(°)	t_G(Å)
Both	HT	>0	0	0	0	0
DMN-D_6	91	−20	9·5 (3)	0·6 (3)	3·7 (4)	0·079 (3)
DMN-H_6	85	−22	11·3 (3)	2·6 (3)	4·9 (4)	0·099 (4)

translated (t_G) out of the symmetry plane; however, the more significant displacement seems to be a rotation (ω) of the molecule about an axis passing through G parallel to the direct cell axis a (Table 4).

The structural modifications occurring at the transition from the HT to the LT form can thus be described to a first approximation by two angular parameters: one (δ) of internal deformation of the molecule, the other (ω) of molecular rotation.

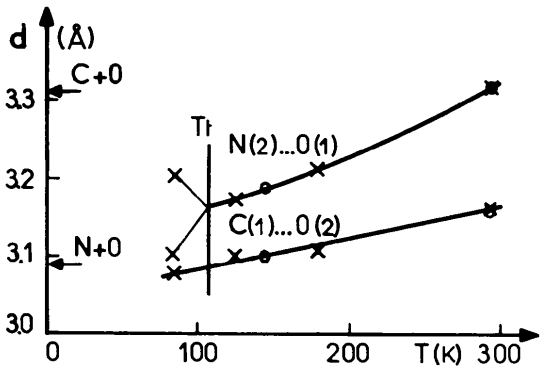

Fig. 7. Intramolecular distances C(1)···O(2) and N(2)···O(1) in DMN-H_6 as a function of temperature (average e.s.d. 0·004 Å). The arrows indicate the value of the sum of the van der Waals radii. O Krebs *et al.* (1979), × structures reported here.

(iv) *Intermolecular interactions*

If initially only the molecules in the (010) plane are considered, a single short intermolecular distance is noted. This is the C(1)···O(2) distance (Fig. 5) between molecules related by the translation along a. Even at room temperature it is shorter [3·166 (5) Å] than the sum of the van der Waals radii and it decreases with temperature (Fig. 7). For molecules of different (010) planes, in the HT form the N–O bonds related by the 2_1 axis are parallel to N(2)···O(1), of 3·32 Å at 293 K and 3·21 Å at 143 K. Krebs *et al.* (1979) raised the possibility of a π-bonding interaction. However, this probably does not play a dominant role since in the LT form the related N–O bonds are no longer parallel leading to two unequal N(2)···O(1) distances (3·10 and 3·21 Å at 85 K), the shorter being close to the van der Waals distance (Fig. 7).

The crystalline cohesion of DMN thus seems to be dominated essentially by the polar nature of the molecule [μ = 4·61 D (~15·4 × 10^{-30} Cm) in solution in dioxane at 293 K (Georges & Wright, 1958)] and by van der Waals forces.

(v) *Thermal motion*

Fig. 8 shows *ORTEP* plots (Johnson, 1970) of thermal-motion ellipsoids of the atoms at several temperatures. The major axis of the thermal ellipsoids is perpendicular to the molecular plane for all non-H atoms. Krebs *et al.* (1979) showed that these large displacements could not be interpreted as a statistical disorder of a non-planar molecule about the symmetry plane, but have a true thermal character. In fact the anisotropy of the thermal ellipsoids, averaged over all six atoms, remains constant when the temperature decreases from 293 to 143 K, whereas the volume of the ellipsoids decreases.

This conclusion is confirmed by neutron results, firstly because this average anisotropy is also the same for the HT structure (125 K, $P2_1/m$) and the LT structures (91 and 85 K, $P2_1/c$), and secondly because the $P2_1/m$ refinement of the 85 K data leads to more elongated ellipsoids than those observed at 125 K.

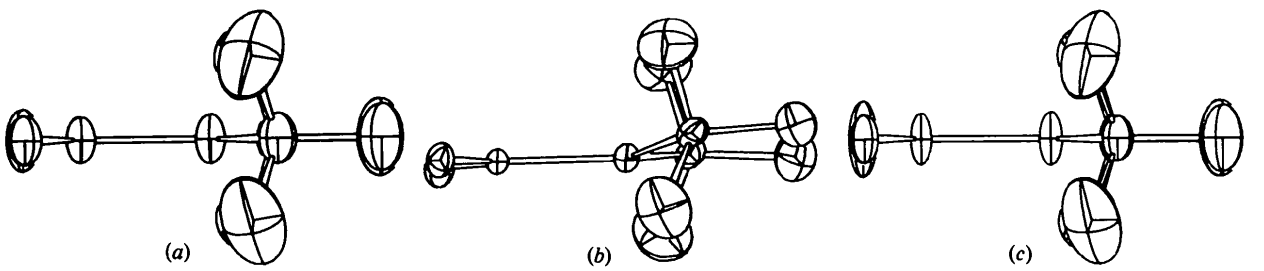

Fig. 8. Atomic thermal-motion ellipsoids (50% probability). The symmetry plane is perpendicular to the plane of the drawing. (*a*) DMN-H_6 125 K, neutrons. (*b*) DMN-H_6 85 K, neutrons ($P2_1/c$ refinement). (*c*) DMN-H_6 85 K, neutrons ($P2_1/m$ refinement).

Table 5. *Cell dimensions of* DMN-H_6 *and* DMN-D_6

E.s.d.'s are given in parentheses. n = neutrons, XR = X-rays.

T (K)	a (Å)	b (Å)	c (Å)	β (°)	V (Å^3)	ρ_c (Mg m^{-3})	Radiation	Diffractometer or reference
Hydrogenated *N,N*-dimethylnitramine								
Room temperature	6·60	6·48	6·13	123·09	219·7	1·362	XR	Costain & Cox (1947)
293 ± 1	6·580 (1)	6·501 (1)	6·129 (1)	123·18 (2)	219·4	1·364	XR	Krebs *et al.* (1979)
293 ± 1	6·587 (2)	6·500 (1)	6·131 (2)	123·13 (2)	219·8	1·361	XR	AED Siemens
242 ± 2	6·576 (2)	6·392 (1)	6·109 (2)	123·49 (2)	215·4	1·389	XR	AED Siemens
206 ± 2	6·568 (2)	6·335 (1)	6·102 (2)	123·42 (2)	211·9	1·412	XR	AED Siemens
191 ± 2	6·566 (2)	6·312 (1)	6·096 (2)	123·48 (2)	210·7	1·420	XR	AED Siemens
181 ± 2	6·564 (2)	6·295 (1)	6·094 (2)	123·53 (2)	209·9	1·426	XR	AED Siemens
164 ± 2	6·558 (2)	6·269 (1)	6·084 (2)	123·58 (2)	208·4	1·436	XR	AED Siemens
143 ± 3	6·557 (1)	6·266 (1)	6·088 (1)	123·54 (2)	208·4	1·436	XR	Krebs *et al.* (1979)
133 ± 3	6·550 (2)	6·232 (1)	6·075 (2)	123·62 (2)	206·5	1·449	XR	AED Siemens
125	6·54	6·23	6·09	123·6	206·6	1·448	XR	AED Siemens
125 ± 0·2	6·560 (4)	6·237 (6)	6·096 (5)	123·66 (5)	207·6	1·441	n	D10 (ILL)
85 ± 0·2	6·531 (6)	6·188 (8)	12·152 (8)	123·69 (5)	408·5	1·465	n	D10 (ILL)
4·2	6·523 (5)	6·165 (5)	12·020 (5)	123·66 (10)	402·3	1·488	XR	Powder
Deuterated *N,N*-dimethylnitramine								
296 ± 0·5	6·583 (2)	6·495 (2)	6·126 (2)	123·17 (1)	219·3	1·454	n	D8 (ILL)
120 ± 0·1	6·555 (8)	6·207 (7)	6·085 (8)	123·74 (6)	205·9	1·549	n	D1B (ILL)
110 ± 0·5	6·543 (2)	6·196 (2)	12·147 (3)	123·73 (1)	409·6	1·557	n	D8 (ILL)
95 ± 0·1	6·560 (6)	6·191 (5)	12·192 (13)	123·82 (5)	411·6	1·549	n	D1B (ILL)
91 ± 0·5	6·535 (1)	6·178 (1)	12·137 (2)	123·76 (1)	407·4	1·565	n	D8 (ILL)
73 ± 0·5	6·531 (1)	6·170 (1)	12·135 (1)	123·78 (1)	406·4	1·569	n	D8 (ILL)
15 ± 0·1	6·524 (2)	6·148 (2)	12·147 (7)	123·87 (3)	405·7	1·576	n	D1B (ILL)

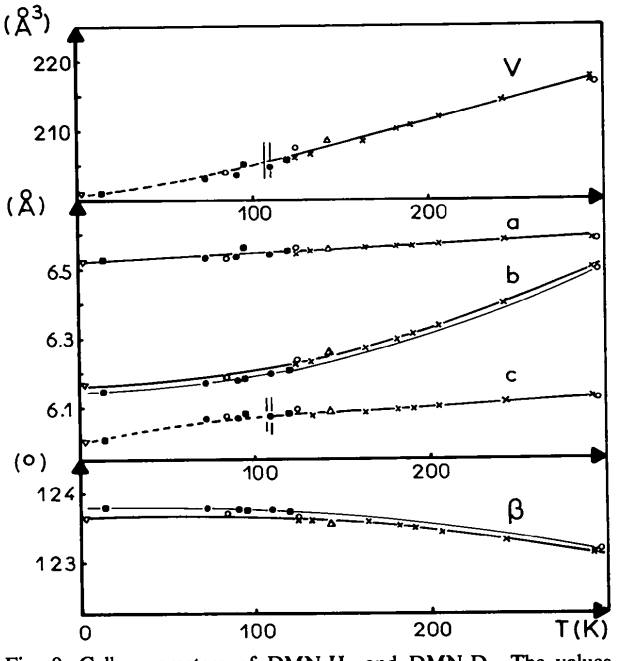

Fig. 9. Cell parameters of DMN-H_6 and DMN-D_6. The values shown for c and V are c and V if $T > T_t$ and $c/2$ and $V/2$ if $T < T_t$. DMN-H_6: heavy lines; △ Krebs *et al.* (1979); × X-rays, single-crystal data; ▽ X-rays, powder data; O neutrons, single-crystal data. DMN-D_6: light lines; ● neutrons, single-crystal data; ■ neutrons, powder data.

(vi) *Thermal expansion*

The changes in the lattice parameters of DMN-H_6 and DMN-D_6 (Table 5 and Fig. 9) as a function of temperature are monotonic in the range 293 to 4·2 K except, of course, for the c parameter which doubles at

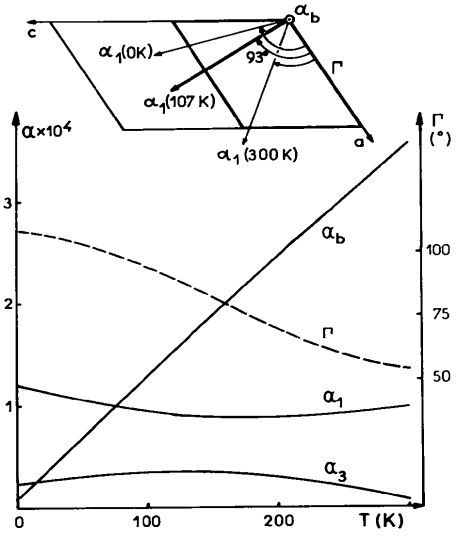

Fig. 10. Main thermal expansions α_1, α_b, α_3 ($\times 10^4$) and angle Γ between directions $\mathbf{a}_1$ and $\mathbf{a}$. The inset shows the direction of the main expansions for temperatures $T = 293$ and 4·2 K.

T_t. However, if the values of c are plotted as c for $T > T_t$ and as $c/2$ for $T < T_t$, the curve thus obtained is also monotonic. It is further to be noted that at all temperatures the lattices of these two compounds have the same a and c parameters, while b and β show differences of approximately 0·3% and 0·1% respectively.

The data for DMN-H_6 were parameterized with second-order polynomials. Starting from these, it is possible to calculate directly the thermal expansion tensor (second-order symmetrical tensor) for any temperature in the range of observation and thus to determine the main expansion values (α_i) and the corresponding orthogonal directions ($\boldsymbol{\alpha}_i$). As DMN crystallizes in the monoclinic system, one of these axes ($\boldsymbol{\alpha}_b$) is parallel to the crystallographic b axis and the two others ($\boldsymbol{\alpha}_1$ and $\boldsymbol{\alpha}_3$) are in the ac plane. The results are shown in Fig. 10.

Discussion

(i) *Cohesion forces*

To attempt a qualitative explanation of the thermal-expansion results for DMN-H_6, it must first be recalled that in the crystals the cohesion forces are essentially of electrostatic and van der Waals types. It is therefore possible to reason on a basis of the following simplified model.

The interatomic contact values (previous section) and the arrangement of the molecules in the lattice (Fig. 5) suggest that the structure of DMN at 293 K is of a layer type. The molecules constitute layers perpendicular to b with a stacking distance of 3·25 Å. In these layers, if each molecule is referred to its equivalent dipole, the existence of dipole chains is observed, with all the dipoles parallel within one chain and all chains parallel, *i.e.* ferroelectric-type organization, within one layer. The chains are parallel to c and spaced by a period a. They are staggered by almost $c/2$ in the c direction (β almost 120°).

The strong temperature dependence of α_b suggests that cohesion forces between layers will weaken rapidly as the temperature increases. However, if the layers are well separated at HT ($\alpha_b \gg \alpha_1 > \alpha_3$) as is shown by the presence of an easy $\langle 010 \rangle$ cleavage, at LT ($\alpha_1 > \alpha_3 > \alpha_b$ at 4 K) the cohesion forces seem to have a more isotropic distribution.

The expansions α_1 and α_3 are, on the contrary, practically independent of temperature (with α_1 = two or three times α_3) but change direction with it. In fact, $\boldsymbol{\alpha}_1$ is practically parallel to [101] at 293 K and is progressively oriented toward the lattice c direction as the temperature decreases. This may be interpreted by noting that [101] (which is the direction of the c_I axis in the old definition of the HT lattice of DMN) is the natural direction of maximum expansion if the dipole chains expand only a little but separate considerably while remaining bonded to one another in the a direction by the $C^{\delta+}\cdots O^{\delta-}$ interaction. At very low temperatures, however, the chains expand more.

Finally, at the transition temperature (T_t = 107 K), α_1 is perpendicular to the cell axis a so that $\boldsymbol{\alpha}_3$, the weakest expansion direction, is practically parallel to this axis and therefore is parallel to the direction of the only strong van der Waals contact in the structure [C(1)···O(2) ≃ 3·08 Å, the value interpolated at 107 K].

(ii) *Long- and short-range order*

In the course of the sample cooling, the observations made in the range 137 to 75 K on the $\bar{3}11$ reflection of DMN-D_6 first of all show the existence of a weak and broad peak of diffuse scattering (p), which disappears toward 110 K in favor of a Bragg peak (P). The latter has full width at half-height smaller and constant, and intensity increasing rapidly with decreasing temperature (Fig. 4).

The change in intensity of the $\bar{3}11$ reflection in the temperature range under consideration seems to be continuous at the level of precision of the measurements. For $T < T_t$, it can be parameterized by a straight line $I^{1/2\beta} = (T_t - T)$ with $\beta \simeq 0{\cdot}27$ and T_t = 110·5 (2) K. These results, however, require confirmation by more accurate observations carried out on several superlattice reflections before the order of the transition can be defined.

The scattering observed for $T > T_t$ may be attributed to short-range order. The corresponding correlation length has been calculated, starting from the width at half-height of the peak (p) on the hypothesis that the resolution of the instrument is given by the width at half-height (independent of temperature) observed for the peak (P) at $T < T_t$. The values thus obtained are 60 Å at 111 K and 20 Å at 137 K.

(iii) *Transition mechanism*

The transition of DMN is of a displacive type, as a soft mode has been observed by Raman spectroscopy (Rey-Lafon, 1979). The value observed for the ratio of scale factors of the superlattice and the main reflections ($k_s/k_m = 1$) and the fact that the ellipsoids of atomic thermal motion present the same anisotropy at 125 and 91 K also agree with this displacive character.

In a molecular crystal such as DMN the potential involved in the phase transition is the sum of intra- and intermolecular potentials.

The intramolecular potential has a single well since the theoretical structure calculations (Farminer & Webb, 1975; Duke, 1978) and experimental data (Bastiansen, 1950; Stolevik & Rademacher, 1969) have

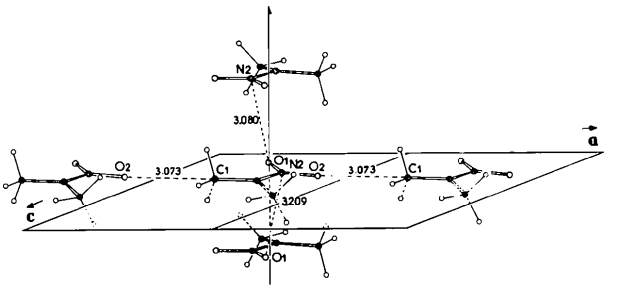

Fig. 11. The main intermolecular interactions (Å) for the 91 K structure. The corresponding average e.s.d. is 0·003 Å.

shown that the most stable conformation is that corresponding to the planar molecule, but the energy required to deform the molecule by an angle δ is probably very low. In these conditions, the distortion responsible for the loss of symmetry must have its origin in molecular interactions.

This distortion, which is described to a first approximation by the parameters δ and ω already defined, is probably due to the combined action of the interactions C(1)···O(2) and N(2)···O(1) (Fig. 11), of which the distances extrapolated to 107 K for the HT form are 3·08 and 3·16 Å respectively. The interaction C(1)···O(2) corresponds to a strong van der Waals contact and associates the molecules in the *a* direction, which is also the direction of the axis of rotation ω. The molecule, which is strongly constrained in the C(1)–N(1)–N(2)–O(2) direction, is deformed at its point of least resistance, N(1), through an angle δ. The van der Waals contact N(2)···O(1) only intervenes to limit the ω rotation.

Therefore, the behavior of the molecule in the LT phase is expected to be the following. When temperature decreases, δ increases while ω will probably change little or even decrease because of the shortening of the *b* axis.

The soft mode associated with the phase transition is therefore certainly a composite one; in this mode the rotation of the whole molecule, defined as ω rotation, must be coupled to an internal component corresponding to the deformation of the molecule out of the symmetry plane (γ_{NN}). Unfortunately, an accurate analysis of the lowest-molecular-frequency domain of the infrared and Raman spectra is made difficult by the weak intensities of several bands. A previous tentative assignment (Trinquecoste, Rey-Lafon & Forel, 1974) must be reconsidered in view of recent results obtained by neutron inelastic scattering on DMN-H_6 at 10 and 127 K (Lassègues & Rey-Lafon, 1979).

A comparison can be made between the mechanism described above and that occurring in other molecular crystals which exhibit a displacive transition. In chloranil, the symmetry-breaking distortion is a rotation of the whole molecule about an axis perpendicular to the molecular plane due to the existence of a strong intermolecular van der Waals contact (C···O = 2·85 Å). In biphenyl, the distortion is the appearance of a torsion angle between the planes of phenyl groups due to the intramolecular repulsion H···H while the crystalline force field tends to make the molecule planar. The phase transition of DMN offers an example of a more complex combination of the roles of intra- and intermolecular forces than those observed for chloranil and biphenyl. Further investigations of this phase transition are in progress.

The authors thank Drs H. Cailleau and J. C. Baudour (Département de Physique Cristalline et Chimie Structurale, Université de Rennes, France) for helpful discussions of this work and Dr J. L. Buevoz (ILL) for help in all the neutron powder experiments.

References

BASTIANSEN, O. (1950). From reference No. 198 of ALLEN, P. W. & SUTTON, L. E. (1950). *Acta Cryst.* **3**, 46–72.

BREE, A. & EDELSON, M. (1977). *Chem. Phys. Lett.* **46**, 500–504.

CAILLEAU, H., BAUDOUR, J. L. & ZEYEN, C. M. E. (1979). *Acta Cryst.* B**35**, 426–432.

CAILLEAU, H., MOUSSA, F. & MONS, J. (1979). *Solid State Commun.* **31**, 521–524.

CLAUDET, G. M., TIPPE, A. & YELON, W. B. (1976). *J. Phys. E*, **9**, 259–261.

COSTAIN, W. & COX, E. G. (1947). *Nature (London)*, **160**, 826–827.

DUKE, B. J. (1978). *J. Mol. Struct.* **50**, 109–114.

ELLENSON, W. D. & KJEMS, J. K. (1977). *J. Chem. Phys.* **67**, 3619–3623.

FARMINER, A. R. & WEBB, G. A. (1975). *J. Mol. Struct.* **27**, 417–421.

FILHOL, A. (1971). Thèse de Docteur Ingénieur. Laboratoire de Cristallographie et de Physique Cristalline, Université de Bordeaux I, 33405 Talence, France.

FILHOL, A., CLÉMENT, C., FOREL, M. T., PAVIOT, J., REY-LAFON, M., RICHOUX, G., TRINQUECOSTE, C. & CHERVILLE, J. (1971). *J. Phys. Chem.* **75**, 2056–2060.

GEORGES, M. V. & WRIGHT, F. (1958). *J. Am. Chem. Soc.* **80**, 1200–1204.

GERMAIN, G., MAIN, P. & WOOLFSON, M. M. (1971). *Acta Cryst.* A**27**, 368–376.

HANSON, D. M. (1975). *J. Chem. Phys.* **63**, 5046–5047.

HOHLWEIN, D. & WRIGHT, A. (1980). *J. Appl. Cryst.* To be published.

International Tables for X-ray Crystallography (1974). Vol. IV. Birmingham: Kynoch Press.

JOHNSON, C. K. (1970). *ORTEP.* Report ORNL-3794. Oak Ridge National Laboratory, Tennessee.

KREBS, B., MANDT, J., COBBLEDICK, R. E. & SMALL, R. W. H. (1979). *Acta Cryst.* B**35**, 402–404.

LAGNIER, R. (1978). Private communication.

LASSÈGUES, J. C. & REY-LAFON, M. (1979). Private communication.

LEHMANN, M. S. & LARSEN, F. K. (1974). *Acta Cryst.* A**30**, 580–584.
REY-LAFON, M. (1979). *J. Chem. Phys.* **71**, 5324–5328.
REY-LAFON, M. & LAGNIER, R. (1975*a*). *C. R. Acad. Sci. Sér. C*, **280**, 547–550.
REY-LAFON, M. & LAGNIER, R. (1975*b*). *Mol. Cryst. Liq. Cryst.* **32**, 13–16.
STEWART, R. F., DAVIDSON, E. R. & SIMPSON, W. T. (1965). *J. Chem. Phys.* **42**, 3175–3187.
STOLEVIK, R. & RADEMACHER, P. (1969). *Acta Chem. Scand.* **23**, 672–682.
TERAUCHI, H., SAKAI, T. & CHIHARA, H. (1975). *J. Chem. Phys.* **62**, 3832–3833.
TRINQUECOSTE, C., REY-LAFON, M. & FOREL, M. T. (1974). *Spectrochim. Acta Part A*, **30**, 813–826.
TROUGHTON, P. G. H. (1969). *Practical Experience in Working with a Siemens Automatic Single-Crystal Diffractometer*, Department of Chemical Crystallography, Imperial College, London SW7, England.
WRIGHT, A. & BERNERON, M. (1980). *Nucl. Instrum. Methods.* To be published.

Acta Cryst. (1980). B**36**, 586–591

Structural Studies of Benzene Derivatives. VIII.* Refinement of the Crystal Structure of *p*-Dinitrobenzene

BY FERNANDA DI RIENZO AND ALDO DOMENICANO

Istituto di Chimica Farmaceutica e Tossicologica, Università di Roma, Città Universitaria, 00185 *Roma and Laboratorio di Strutturistica Chimica del CNR 'Giordano Giacomello',* 00016 *Monterotondo Stazione, Italy*

AND LODOVICO RIVA DI SANSEVERINO

Istituto di Mineralogia e Petrografia, Università di Bologna, Piazza San Donato 1, 40127 *Bologna, Italy*

(*Received* 7 *August* 1979; *accepted* 18 *September* 1979)

Abstract

$C_6H_4N_2O_4$ is monoclinic, space group $P2_1/n$, with a = 11·137 (2), b = 5·461 (1), c = 5·684 (3) Å, β = 92·22 (4)°, Z = 2. The final R is 0·0408 for 559 independent counter intensities. The benzene ring has *mmm* symmetry within experimental error. The distortions from 6/*mmm* symmetry are quite marked, and involve bond lengths as well as angles; they testify to the strong σ-electron-withdrawing character of the substituent. The value of the internal angle at the *ipso* atom, α_{NO_2} = 123·4 (1)°, is in good agreement with values reported for other molecules where the nitro group is *para* to a π acceptor.

Introduction

The structures of several *para*-substituted derivatives of nitrobenzene, *p*-X–C_6H_4–NO_2, are being studied in our laboratories to investigate the effect of X on the ring distortions caused by the nitro group. Results have been presented for *p*-nitrobenzoic acid (Colapietro & Domenicano, 1977) and *p*-nitrobenzamide (Di Rienzo, Domenicano & Foresti Serantoni, 1977); here we report the structure of *p*-dinitrobenzene. A preliminary communication has been given (Colapietro, Di Rienzo, Domenicano, Portalone & Riva di Sanseverino, 1977).

The beautiful, well formed crystals of *p*-dinitrobenzene have stimulated the interest of X-ray crystallographers for half a century. Pioneering work was done by Hertel & Schneider (1930), Banerjee (1934), and James, King & Horrocks (1935): essentially correct atomic coordinates are presented in the last paper. Two independent studies by Fourier methods were performed later: one based on a set of three-dimensional photographic data (Llewellyn, 1947, but see also Abrahams, 1950), the other on two-dimensional data (Abrahams & Robertson, 1947). Several years later Trotter (1961) used Llewellyn's data to refine the structure by $(F_o - F_c)$ syntheses. The refinement converged to R = 0·19, and led to e.s.d.'s of the atomic positions of 0·02 Å. To our knowledge, no further work on the crystal structure of *p*-dinitrobenzene has been reported. A gas-phase electron diffraction study has been published (Sadova, Popik, Vilkov, Pankrushev & Shlyapochnikov, 1974).

Experimental

Pale-yellow prisms were grown from an acetone solution of the commercial product (Fluka). Oscillation

* Part VII: Colapietro, Domenicano & Portalone (1980).

0567-7408/80/030586-06$01.00